Bioconjugate Chemistry

Article

pubs.acs.org/bc

Functional Characterization of Fluorescent Hepcidin

Franz Dürrenberger,[§] Vincenzo Abbate,[†] Yongmin Ma,[†] Maria C. Arno,[†] Dareen Jaiash,[†] Archna Parmar,[†] Victoria Marshall,[†] Gladys O. Latunde-Dada,[‡] Tina Zimmermann,[§] David Senn,[§] Patrick Altermatt,[§] Vania Manolova,[§] Robert C. Hider,[†] and Sukhvinder S. Bansal*[,†]

[†]Chemical Biology Group, Institute of Pharmaceutical Sciences, and [‡]Nutrition and Diabetes Research Group, King's College London, Franklin-Wilkins Building, 150 Stamford Street, London SE1 9NH, U.K.

[§]Vifor Pharma, Chemical and Preclinical Research and Development, Rechenstrasse 37, CH-9001 St. Gallen, Switzerland

ABSTRACT: Hepcidin is a peptide hormone that regulates homeostasis in iron metabolism. It binds to the sole known cellular iron exporter ferroportin (Fpn), triggers its internalization, and thereby modulates the efflux of iron from cells. This functional property has been adopted in this study to assess the bioactivity and potency of a range of novel fluorescent hepcidin analogues. Hepcidin was selectively labeled with 6-carboxyfluorescein (CF) and 6-carboxytetramethylrhodamine (TMR) using Fmoc solid phase peptide chemistry. Internalization of Fpn by hepcidin was assessed by high-content microscopic analysis. Both K18- and M21K-labeled hepcidin with TMR and CF exhibited measurable potency when tested in cultured MDCK and T47D cells expressing human ferroportin. The bioactivity of the labeled hepcidin varies with the type of fluorophore and site of attachment of the fluorophores on the hepcidin molecule.

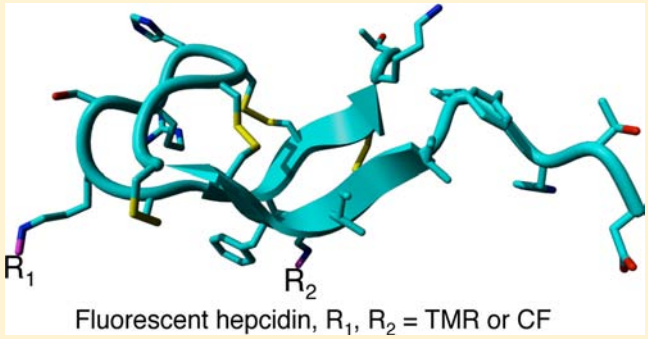

Fluorescent hepcidin, R_1, R_2 = TMR or CF

INTRODUCTION

Hepcidin, a peptide hormone produced primarily in the hepatocyte, plays a pivotal role in the regulation of systemic iron homeostasis in mammals.[1,2] Several studies[3−5] have demonstrated a reciprocal relationship between hepatic hepcidin mRNA expression and efflux of iron into circulation from either the intestine or the reticuloendothelial system. Hepcidin levels increase when iron stores are elevated or during inflammation and decrease during conditions of anemia, hypoxia, and pregnancy, as well as in hypotransferrinemic mice.[6] Hepcidin regulates serum iron homeostasis by triggering the degradation of Fpn.[7] Hepcidin interacts with Fpn to induce the latter's internalization, followed by ubiquitination and degradation. This role ablates the function of Fpn in the enterocytes, macrophages, and placenta. The regulation of hepcidin expression has been delineated from studies using transgenic mouse models in the iron BMP/SMAD and inflammatory JAK/STAT3 signaling pathways.[8,9] However, recent studies indicate Fpn internalization requires ferroportin lysines and not tyrosine or JAK/STAT.[10]

Hepcidin is synthesized as a preprohepcidin of 84 amino acids, which is cleaved into the 60-amino acid prohepcidin and processed further into an active peptide of 25 amino acids.[11] The active 25-amino acid amphipathic hepcidin peptide is rich in β-sheet structure, which is stabilized by four conserved intramolecular disulfide bridges into a hairpin configuration.[12,13] At present, most studies of tissue localization and trafficking of hepcidin rely upon fluorescently tagged Fpn or radioiodinated hepcidin. The intrinsic resolution limit of the radiolabeling approach precludes monitoring these processes with good morphological and molecular detail. In comparison, fluorescence labeling coupled with optical imaging offers submicrometer level resolution and is noninvasive. In addition, a specific spectroscopic signature of the fluorescent label allows efficient visualization of cell morphology and autofluorescence background, thereby elevating the sensitivity toward visible single ligand−receptor events.

To the best of our knowledge, there are three prior reports of fluorescent hepcidins, which were either nonselectively labeled with Texas Red *N*-hydroxysuccinimide ester[14] or site-specifically labeled at position 21 with the red fluorescent dye azido-PEG4-Fluoro525 using click chemistry[15] and rhodamine green labeled via an aminohexyl spacer to the ε-amino group of a lysine residue.[10] We have previously reported the application of fluorescent hepcidin.[16]

In this paper, we report the synthesis of hepcidin selectively labeled with 6-carboxyfluorescein (CF) at $N^{\varepsilon 18}$ (K18-CF) and [Lys^{21}] $N^{\varepsilon 21}$ (M21K-CF) or with 6-carboxytetramethylrhodamine (TMR) at [Lys^{21}] $N^{\varepsilon 21}$ (M21K-TMR), using solid phase peptide chemistry, in addition to studies of their folding and functional characterization.

Received: March 5, 2013
Revised: July 1, 2013
Published: July 26, 2013

dx.doi.org/10.1021/bc400121x | *Bioconjugate Chem.* 2013, 24, 1527−1532

EXPERIMENTAL PROCEDURES

Synthesis of Hepcidin. The Fmoc amino acid derivatives were obtained from Bachem AG (Bubendorf, Switzerland). Lysine was protected using (4,4-dimethyl-2,6-dioxocyclohex-1-ylidene)ethyl (Dde) at lysine 18 (K18) or by replacement of methionine 21 with lysine (M21K). Peptide synthesis was conducted on a CEM Liberty 1 microwave peptide synthesizer with Fmoc-Thr(tBu)-Trt-Resin on a 0.2 mmol scale. All deprotection reactions were conducted with 20% piperidine in dimethylformamide (v/v). Acylation reactions were conducted using 2-(6-chloro-1*H*-benzotriazol-1-yl)-1,1,3,3-tetramethylaminium hexafluorophosphate (HCTU) (0.78 mmol) in the presence of 2,4,6-collidine (1.6 mmol) for 10 min using a microwave power of 25 W. Cysteine and histidine were activated with diisopropylcarbodiimide (0.8 mmol) and ethyl cyano(hydroxyimino) acetate (0.8 mmol). Boc-Asp (OtBu)-OH was incorporated at the N-terminus.[17]

Upon completion of the synthesis, the peptide resin (400 mg, 69 μmol) was treated with 15 mL of hydrazine hydrate in dimethylformamide (2%, v/v) to selectively remove the Dde group. The free amino group was acylated with either 6-carboxyfluorescein (65 mg, 173 μmol) or 6-carboxytetramethylrhodamine (45 mg, 104 μmol), diisopropylcarbodiimide (27 μL, 173 μmol), and ethyl cyano(hydroxyimino) acetate (25 mg, 173 μmol) in 2 mL of dimethylformamide over 18 h.

The labeled peptide resin (400 mg, 69 μmol) was cleaved from the solid support and simultaneously deprotected using trifluoroacetic acid, phenol, water, thioanisole, and 3,6-dioxo-1,8-octanedithiol (82.5/5/5/5/2.5) for 4 h. The peptide was then dissolved in 100 mL of reducing buffer consisting of Tris hydrochloride (0.5 M), EDTA (0.1 mmol), and GdnHCl (6 M) at pH 8.8 and reduced with excess dithiothreitol (53 mg, 345 μmol). The fluorescent peptide solution was acidified to pH 2.5 and then purified by preparative high-performance liquid chromatography (HPLC) on a Vydac 218TP54 peptide and protein column (2.5 cm × 30 cm). The folding buffer (6.8 L) consisted of ammonium bicarbonate (100 mmol), EDTA (0.1 mmol), guanidinium hydrochloride (GdmHCl) (2 mol), reduced glutathione (2.10 g, 6.9 mmol), and oxidized glutathione (0.42 g, 0.69 mmol). The purified reduced peptide was dissolved in 100 mL of folding buffer containing 6 M GdmHCl and added to the bulk of the folding buffer. Oxidative folding was conducted for 48 h, and the resulting peptide was purified by preparative HPLC. The major peaks obtained were further purified on a Vydac peptide and protein 218 TP54 semipreparative column (1. 0 cm × 30 cm), and the resulting fractions were analyzed by HPLC and mass spectrometry (MS).

Mass Spectrometry. Mass spectrometry analysis of the peptides was conducted using matrix-assisted laser desorption ionization on a Bruker Autoflex instrument. An Nd:YAG laser (355 nm) was used to irradiate the sample. The instrument was calibrated with a range of peptides covering the mass range of 500−4000 Da. Samples were prepared on an Anchor Chip with a saturated solution of α-cyano-4-hydroxycinnamic acid as the matrix in a mixture of acetonitrile and 0.1% trifluoroacetic acid.

Ferroportin Internalization Assay. A stable cell line [Madin-Darby canine kidney (MDCK)] was generated, which constitutively expressed human ferroportin (Fpn) fused at its C-terminus to the HaloTag protein (Promega Corp.). The internalization of Fpn was traced by labeling these cells with the fluorescent HaloTag-TMR (tetramethylrhodamine) ligand, which covalently attached to the HaloTag protein; 30000 Fpn-HaloTag MDCK cells were seeded in 100 μL of DMEM (Dulbecco's modified Eagle's medium with 10% fetal bovine serum (FBS) containing 1% penicillin, 1% streptomycin, and 450 μg/mL G-418) per well of 96-well microplates (Micro-Clear, Greiner, catalog no. 655096). After overnight incubation at 37 °C and 5% CO_2, the HaloTag-TMR ligand (Promega, catalog no. G8251) was added to the cells to a final concentration of 2 μmol/L and incubated for 15 min at 37 °C and 5% CO_2. Cells were washed with phosphate-buffered saline (PBS); 100 μL of DMEM was added, and the cells were incubated for 30 min at 37 °C and 5% CO_2. The medium was replaced with 50 μL of fresh DMEM, and 50 μL of the test compound diluted in DMEM was added. Hepcidin dose−response experiments were conducted with either 8- or 11-concentration dilution series of CF-hepcidin analogues and reference hepcidin (Bachem, catalog no. H-5926) spanning concentration ranges of 4 μmol/L to 0.2 nmol/L for CF-hepcidin analogues and 2 μmol/L to 0.03 nmol/L for the reference hepcidin. Dose−response experiments were conducted with either three or four wells per peptide concentration for 8- or 11-concentration dilution series, respectively. After overnight incubation at 37 °C and 5% CO_2, 25 μL of Draq5 (Biostatus, catalog no. DR51000) was added to a final concentration of 2.5 μmol/L and the mixture incubated for 10 min at 37 °C and 5% CO_2 to stain cell nuclei. After the cells had been washed with 200 μL of DMEM without phenol red (GIBCO, catalog no. 11880), cells were fixed in 100 μL of 4% paraformaldehyde (PFA) (Electron Microscopy Sciences, catalog no. 15710-S) in PBS for 15 min at room temperature. The PFA solution was removed; cells were washed with PBS, leaving 100 μL/well, and plates were sealed with foil plate seal. TMR (excitation at 520−550 nm, emission at 560−630 nm, and exposure time of 1000 ms) and Draq5 (excitation at 620−640 nm, emission at 650−760 nm, and exposure time of 200 ms) fluorescence images were acquired using the Operetta high-content screening system (Perkin-Elmer) using a 20× long working-distance objective. Four pictures were acquired per well and fluorescence channel covering ∼2000 cells/well. The acquired image data were imported into the Columbus image data storage and analysis system (Perkin-Elmer) for analysis. Image analysis included detection of nuclei (Draq5 fluorescence) and definition of the cytoplasmic region followed by application of the Ridge SER algorithm to analyze the texture of the TMR fluorescence in the cytoplasmic region as a quantitative measure of subcellular localization of ferroportin. High TMR SER Ridge values correlated with Fpn localized to the cell surface and low TMR SER Ridge values with the absence of Fpn from the cell surface. Relative values for Fpn internalization in percent were calculated as follows: Fpn internalization (%) = [1 − (SER Ridge − average of SER Ridge of 1000 nmol/L hepcidin)/(average of SER Ridge of 0 nmol/L hepcidin − average of SER Ridge of 1000 nM hepcidin)] × 100. EC_{50} values were calculated with the relative Fpn internalization data using "log(agonist) vs response" curve fitting in Prism 5 (GraphPad Software Inc., version 5.02). For each data set, the fit of the "log(agonist) vs response (three parameters)" model was compared to the fit of the "log(agonist) vs response − variable slope (four parameters)" model, and the EC_{50} data of the preferred model were used.

Hepcidin Internalization Assay. T47D cells (80000) were seeded in 100 μL of DMEM/well of 96-well MicroClear plates, and where indicated, Fe(III)-NTA (nitrilotriacetic acid)

was added to a final concentration of 100 μM to induce expression of endogenous human ferroportin. After overnight incubation at 37 °C and 5% CO_2, the medium was replaced with fresh DMEM and dilution series of unlabeled hepcidin spanning a concentration range of 2 μmol/L to 0.1 nmol/L were added in triplicate. T47D cells were preincubated with unlabeled hepcidin at 37 °C and 5% CO_2 for 15 min before M21K-TMR- or K18-CF-hepcidin was added to a final concentration of 25 or 150 nmol/L, respectively. Cells were incubated in a total volume of 50 μL at 37 °C and 5% CO_2 for 2 h, then washed several times with DMEM without phenol red, and fixed in 100 μL of 4% PFA in PBS for 15 min at room temperature. After removal of the PFA solution, cells were washed with PBS, leaving 100 μL/well, and then 5 μL of 10 μg/mL Hoechst 33342 (Invitrogen, catalog no. H3570) was added; cells were incubated for 10 min at room temperature to stain cell nuclei and the plates sealed with foil plate seal. TMR (excitation at 530−550 nm, emission at 575−625 nm, and exposure time of 400 ms) or CF (excitation at 460−495 nm, emission at 510−550 nm, and exposure time of 300 ms) and Hoechst 33342 (excitation at 360−370 nm, emission at 420−460 nm, and exposure time of 10 ms) fluorescence images were acquired using a ScanR plate imager (Olympus) with a 20× high NA objective. Four pictures were acquired per well and fluorescence channel covering ~1500 cells/well. The acquired image data were analyzed with the ScanR image analysis software. Image analysis included detection of nuclei (Hoechst 33342 fluorescence), identification of cell-associated regions, application of a virtual channel, and thresholding for rolling-ball-type background reduction, followed by application of the Sum(Mean) algorithm to measure the TMR or CF fluorescence associated with cells as a quantitative measure of internalized fluorescent hepcidin analogues. IC_{50} values were calculated with the Sum(Mean) raw data as described for the ferroportin internalization assay.

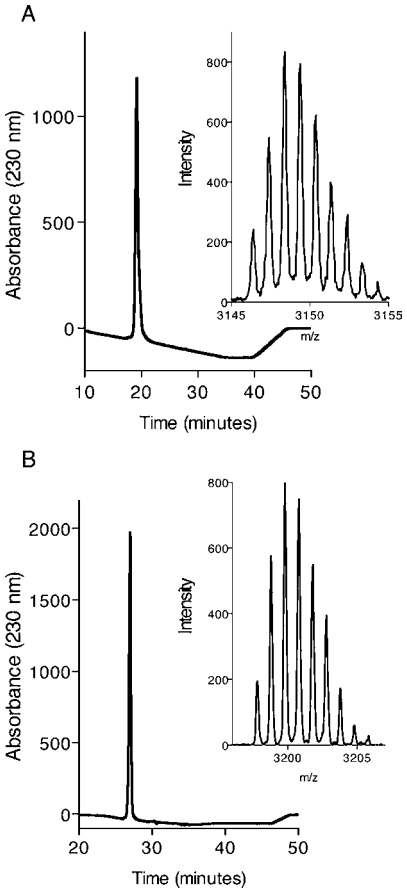

Figure 1. RP-HPLC and MALDI-TOF MS (inset) of (A) K18-CF-hepcidin and (B) M21K-TMR-hepcidin. Conditions: Jupiter C18 column (2.1 mm × 150 mm, pore size of 300 Å, particle size of 5 μm), buffer A (0.1% aqueous TFA), buffer B (0.1% TFA in CH_3CN), flow rate of 0.2 mL/min, gradient from 20 to 90% B over 30 min.

RESULTS

Synthesis of Fluorescently Labeled Hepcidin. The linear peptides were successfully prepared, and the Dde group was selectively removed at K18 or M21K and labeled with both fluorophores. The synthesized 6-tetramethylrhodamine- or 6-carboxyfluorescein-labeled hepcidin was purified by preparative HPLC, and the fractions were analyzed by HPLC and MALDI-TOF MS (Figure 1). K18-TMR-hepcidin and M21K-CF-hepcidin were prepared and characterized in a similar fashion. Typically, from 70 μmol of peptide resin, we obtained 3 μmol of the purified homogeneous peptide, a yield of 5%.

Ferroportin Internalization Activity of the Synthetic CF-Hepcidin Analogues. Functional characterization of the two CF-labeled forms of hepcidin, each derived from either K18 or M21K labeling, was based on their potency to internalize and degrade ferroportin in a cellular assay. A stable MDCK cell line with constitutive expression of human ferroportin fused at its C-terminus to the HaloTag protein was used. Internalization of the Fpn-HaloTag fusion protein was followed in these cells by staining with the fluorescent HaloTag-TMR ligand, which covalently attached to the HaloTag protein. Imaging with fluorescence microscopy revealed cell surface localization of Fpn in the absence of hepcidin and a lack of Fpn surface staining in the presence of hepcidin (see Figure 2a). Image analysis algorithms were used to quantify the membrane fluorescence associated with the Fpn-HaloTag fusion protein. This assay permitted a quantitative evaluation of Fpn internalization potencies of the two CF-hepcidin analogues compared to that of unmodified synthetic reference hepcidin. Representative dose−response curves for M21K-CF-hepcidin, K18-CF-hepcidin, and unmodified hepcidin are shown in Figure 2b. Hepcidin dose−response MDCK assays were repeated several times with M21K-CF-hepcidin (n = 8), K18-CF-hepcidin (n = 6), and unmodified hepcidin (n = 12). While commercially synthesized hepcidin from Bachem effectively internalized and degraded ferroportin with an EC_{50} of 8.6 ± 3.8 nmol/L (average ± standard deviation), K18-CF-hepcidin exhibited an EC_{50} of 34.1 ± 18.8 nmol/L. M21K-CF-hepcidin exhibited an EC_{50} of 78.1 ± 37.0 nmol/L. Thus, the CF modification at M21K led to a 9-fold reduction in Fpn internalization potency in this assay, whereas attachment of the CF fluorophore to lysine at position 18 interfered less with bioactivity and resulted in a 4-fold lower potency compared to that of unmodified hepcidin.

Internalization of Synthetic CF- and TMR-Hepcidin Analogues into T47D Cells. In the MDCK assay that was employed to determine the potency of the two CF-hepcidin analogues, a TMR-HaloTag ligand was used to label ferroportin and quantify its internalization upon hepcidin treatment. The TMR fluorescence of the M21K-TMR-hepcidin interfered with the detection of ferroportin in the MDCK assay. Therefore, internalization of fluorescent hepcidins into T47D cells was assessed to determine the bioactivity of the TMR-labeled

dx.doi.org/10.1021/bc400121x | Bioconjugate Chem. 2013, 24, 1527−1532

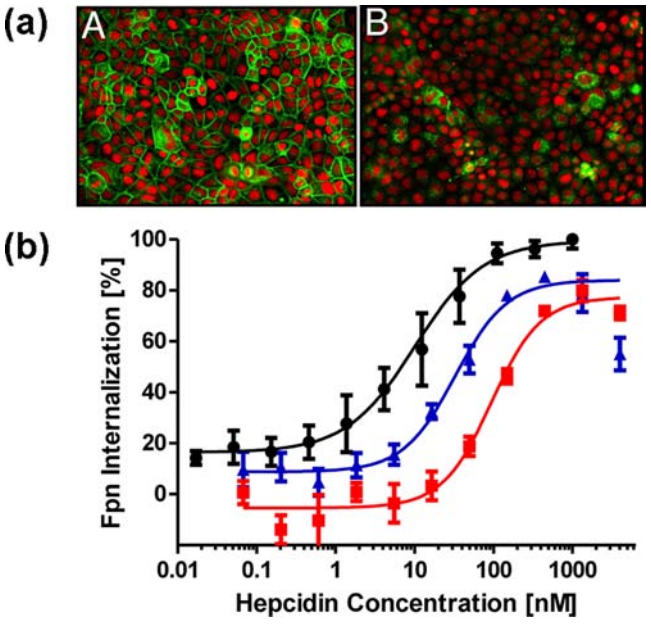

Figure 2. Ferroportin internalization potencies of CF-hepcidin analogues (M21K and K18) compared to that of unmodified reference hepcidin. (a) MDCK cells expressing a human ferroportin-HaloTag fusion protein were used to quantify hepcidin-induced internalization of ferroportin. Cells were stained with the HaloTag- TMR ligand (green) and incubated overnight with 0.2 μmol/L hepcidin (B) or were not treated with hepcidin (A). Draq5 (red) was used for staining of cell nuclei. Binding of the HaloTag-TMR ligand to the HaloTag reporter protein visualized ferroportin localization predominantly at the plasma membrane in the absence of hepcidin treatment (A), whereas relocalization to intracellular compartments and degradation of Fpn were observed for hepcidin-treated cells (B). Images were acquired with a ScanR plate imager (Olympus) at 20× magnification. (b) MDCK cells expressing the Fpn-HaloTag fusion protein were exposed to increasing concentrations of M21K-CF-hepcidin (red curve with squares), K18-CF-hepcidin (blue curve with triangles), and unmodified reference hepcidin (black curve with circles). Subcellular localization of ferroportin was quantified by image analysis. Mean and standard deviation data are shown (n = 4). The relative dose−response data were fit, and EC_{50} values were calculated as follows: 93.8 nmol/L (95% confidence interval of 73.8−119.3 nmol/L) for M21K-CF-hepcidin, 32.7 nmol/L (95% confidence interval of 26.1−40.9 nmol/L) for K18-CF-hepcidin, and 10.1 nmol/L (95% confidence interval of 7.5−13.5 nmol/L) for the reference hepcidin.

hepcidin and to compare it to the potency of CF-hepcidin derivatives in the same assay. T47D is a human breast epithelial tumor cell line that was shown to express Fpn endogenously at the cell surface and that treatment with hepcidin led to internalization and degradation of Fpn.[10] Treatment of T47D cells with M21K-TMR-hepcidin (Figure 3A) or K18-CF-hepcidin (Figure 3C) resulted in the respective cell-associated fluorescence. Part of the cell-associated fluorescence was due to nonspecific binding and/or internalization of the fluorescent hepcidins as revealed by preincubation of T47D cells with 2 μmol/L unlabeled hepcidin before the addition of 25 nmol/L M21K-TMR-hepcidin (Figure 3B) or 150 nmol/L K18-CF-hepcidin (Figure 3D). Quantification of cell-associated fluorescence revealed signal to background ratios of 4.5 and 2.2 for TMR- and CF-hepcidin, respectively, demonstrating that there was more unspecific binding and uptake of the CF-labeled hepcidin and that the TMR-labeled hepcidin derivative is therefore better suited for this type of cellular analysis.

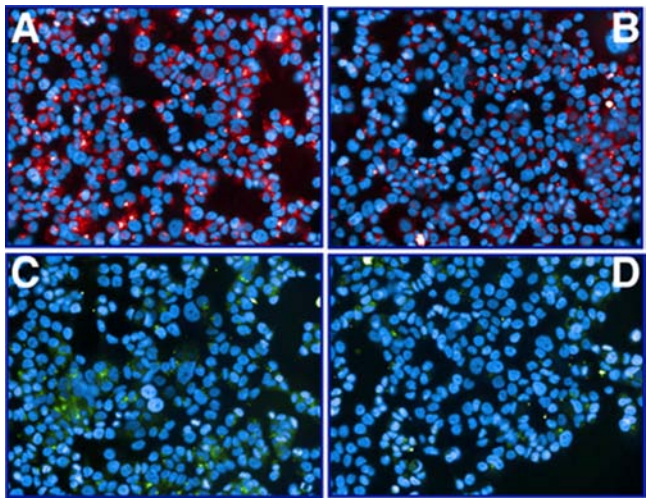

Figure 3. Internalization of CF-hepcidin and TMR-hepcidin analogues in T47D cells with endogenous expression of human ferroportin. T47D cells were grown in the presence of 100 μmol/L Fe(III)-NTA to increase the level of expression of endogenous ferroportin and incubated for 2 h with M21K-TMR-hepcidin (A and B) or K18-CF-hepcidin (C and D). To determine the amount of unspecific binding of the fluorescent hepcidins to T47D cells, cells were incubated for 15 min with 2 μmol/L unlabeled hepcidin prior to the addition of the fluorescent hepcidins (B and D). Cell nuclei were stained with Hoechst 33342 (blue), and TMR (red) and CF (green) fluorescence images were acquired with a ScanR plate imager (Olympus) at 20× magnification.

Dose−response competition experiments were conducted to compare the bioactivities of K18-CF-hepcidin and M21K-TMR-hepcidin. T47D cells were preincubated with dilution series of unlabeled hepcidin prior to the addition of K18-CF-hepcidin or M21K-TMR-hepcidin; fluorescence images were quantitated, and IC_{50} competition values of unlabeled hepcidin were calculated for both fluorescent derivatives. Both M21K-TMR-hepcidin and K18-CF-hepcidin gave very similar competition IC_{50} values of 29.2 ± 7.9 nmol/L (n = 4) and 29.0 ± 2.8 nmol/L (n = 2), respectively, in independent experiments with T47D cells gown in the presence of 100 μmol/L Fe(III)-NTA to increase the level of Fpn expression. Comparable IC_{50} values were also obtained with T47D cells that were grown in the absence of an additional iron source: 35.8 ± 6.4 nmol/L for M21-TMR-hepcidin (n = 2) and 27.2 ± 3.9 nmol/L for K18-CF-hepcidin (n = 2). A representative hepcidin competition experiment is shown in Figure 4. Taken together, these results indicate that M21-TMR- and K18-CF-hepcidin have very similar bioactivities. A summary of the potencies of the fluorescent hepcidin is shown in Table 1.

■ DISCUSSION

Since the discovery of hepcidin and its function in regulating Fpn levels, several studies have employed fluorescence imaging to explore the association of the peptide and the iron efflux protein. Cells expressing endogenous Fpn and transgenic Fpn-GFP protein have been used to study the interaction of hepcidin and ferroportin. The nature, characteristics, and binding kinetics of hepcidin and Fpn are matters of considerable interest in the field of iron metabolism.

This study employed Fmoc solid phase peptide chemistry to synthesize two forms of fluorescently labeled hepcidin. The fluorescently labeled hepcidin was unambiguously labeled by

dx.doi.org/10.1021/bc400121x | Bioconjugate Chem. 2013, 24, 1527−1532

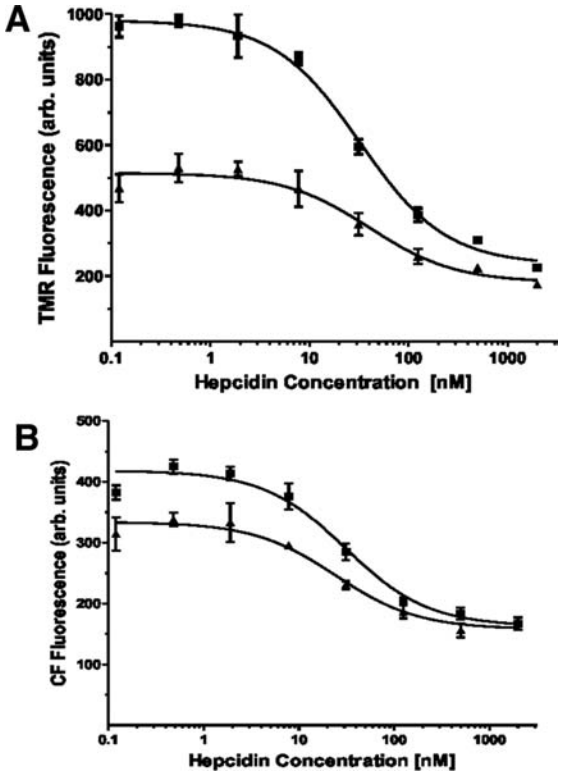

Figure 4. Dose-dependent competition of fluorescent hepcidin internalization in T47D cells by preincubation with unlabeled hepcidin. T47D cells were grown in the absence (▲) or presence (■) of 100 μmol/L Fe(III)-NTA to increase the level of expression of endogenous ferroportin. Before the addition of M21K-TMR-hepcidin (A) or K18-CF-hepcidin (B), T47D cells were incubated with increasing concentrations of unlabeled hepcidin for 15 min. Two hours after the addition of the fluorescent hepcidins, cells were washed and fixed, and fluorescence images were taken. Cell-associated TMR (A) or CF (B) fluorescence was quantified. Preincubation with unlabeled hepcidin resulted in dose-dependent inhibition of internalization of the fluorescent hepcidin derivatives. Mean and standard deviation data are shown (n = 3).

Table 1. Summary of Bioactivities of Fluorescent Hepcidin Derivatives in the Ferroportin and Hepcidin Internalization Assay[a]

		IC_{50} (nmol/L)[c]	
hepcidin peptide	EC_{50} (nmol/L)[b]	without Fe(III)-NTA[d]	with Fe(III)-NTA[d]
unlabeled hepcidin (Bachem)	8.6 ± 3.8 (n = 12)	nd[e]	
M21K-CF-hepcidin	78.1 ± 37.0 (n = 8)	nd[e]	
K18-CF-hepcidin	34.1 ± 18.8 (n = 6)	27.2 ± 3.9 (n = 2)	29.0 ± 2.8 (n = 2)
M21K-TMR-hepcidin	nd[e]	35.8 ± 6.4 (n = 4)	29.2 ± 7.9 (n = 2)

[a]Means ± standard deviations of independent experiments are shown, and the number of experiments is indicated. [b]Ferroportin internalization assay (MDCK). [c]Hepcidin internalization assay (T47D). [d]T47D cells were grown in the absence or presence of 100 micro mol/L Fe(III)-NTA to increase the level of expression of endogenous Fpn. [e]Not determined.

employing an orthogonal protecting strategy during solid phase synthesis; the groups were selectively deprotected, and the label was introduced prior to peptide folding. The site of attachment of the fluorescent label is important as this can affect the conformation, solubility, folding, and biological activity of the peptide. The N-terminus of hepcidin is conserved in nature with human, chimp, porcine, and bovine hepcidin having a DTHFPICIF N-terminal sequence. Furthermore, hepcidin 20 and hepcidin 22, which were isolated from urine, are not active.[12] Thus, the N-terminus is not a suitable site for label attachment. In addition, the cysteines are not suitable candidates for modification by virtue of their structural role. Of the eight remaining amino acids, we excluded the two glycines because they may be necessary to induce turns in the peptide structure; for example, G20F hepcidin failed to fold,[18] although G12D has activity comparable to that of native hepcidin.[11] Of the three remaining segments, H15–K18 (HRSK), M21, and K24 and T25, the first of these is the least conserved region of the hepcidin molecule, and labeling of the basic residues was considered. However, it was reasoned that such modification would reduce the solubility of the peptide. In the last region, K24 and T25 are also conserved in most species, so modification is likely to have a major influence on activity. In contrast, M21 was considered to be a good candidate, because although the character of this position is conserved, it is occupied by a range of hydrophobic amino acids, including Ile, Leu, and Trp. Furthermore, M21Y hepcidin has activity comparable to that of native hepcidin.[11,19,20] In this study, M21 was replaced with K and the ε-amino group was subsequently selectively labeled so the net charge of hepcidin would not be affected. K18 hepcidin was labeled for comparative purposes.

The activities of the CF-labeled fluorescent hepcidins were evaluated on the basis of their potency in internalizing Fpn into MDCK cells. K18-CF fluorescent hepcidin was found to be highly active in internalizing Fpn with an approximate 4-fold decrease in potency compared to that of unmodified synthetic hepcidin. However, attachment of the CF moiety to a lysine at position 21 led to a 9-fold loss of internalization potency. The internalization potencies of K18-CF- and M21K-TMR-hepcidins were compared in a competition assay with that of unlabeled hepcidin for uptake of the fluorescent peptides into T47D cells. The internalization of both M21K-TMR- and K18-CF-hepcidin was effected with very similar IC_{50} values, indicating comparable bioactivity of these two fluorescent hepcidin derivatives. It is possible that the attachment of the carboxyfluorescein moiety to hepcidin influences the secondary structure and the kinetics of binding to Fpn more than the TMR fluorophore.

T47D cells have endogenous levels of Fpn expression, which can be enhanced by pretreating the cells with iron. Incubation overnight with iron did not have any adverse effect on either the bioactivity or the function of fluorescent hepcidins (Figure 4). The fluorescent hepcidins described in this publication allow the use of endogenous Fpn for the characterization of hepcidin analogues. M21K-TMR-hepcidin is, however, beneficial in microscopic analysis of the interaction of hepcidin with endogenous Fpn because of the weaker nonspecific binding to and internalization into T47D cells compared to those of K18-CF-hepcidin (Figure 3).

Fluorescent hepcidin will enhance further studies of hepcidin–Fpn binding characteristics, localization, and optical monitoring in cells and organisms. A recent study[19] used the site-specifically labeled Fluor525-hepcidin[15] to trace internalization of ferroportin fused to the small luciferase protein

dx.doi.org/10.1021/bc400121x | Bioconjugate Chem. 2013, 24, 1527–1532

NanoLuc.[19] Moreover, treatment of cells expressing GFP-tagged ferroportin with Fluor525-hepcidin revealed colocalization of red (Fluor525-hepcidin) and green (Fpn-GFP) fluorescence, indicating that hepcidin and ferroportin accumulate in related intracellular compartments upon hepcidin-triggered endocytosis of Fpn. However, no such colocalization was observed after incubation of cells that expressed the hepcidin-resistant C326S mutant version of Fpn-GFP with Fluor525-hepcidin. Additionally, co-expression of NanoLuc-tagged wild-type Fpn and GFP-tagged hepcidin-insensitive mutant (C326S) Fpn revealed that the mutant had no influence on hepcidin-induced internalization of wild-type Fpn. The exact molecular mechanisms of hepcidin−Fpn interactions in different tissues *in vivo* are still speculative and uncharacterized. However, in a recent *in vitro* cell culture study,[20] hepcidin was labeled with Texas Red succinimidyl ester (TR-hepcidin) to investigate the intracellular fate of the peptide. This study demonstrated that TR-hepcidin colocalized with Fpn-GFP in intracellular vesicles, suggesting that hepcidin internalizes when bound to Fpn. Furthermore, the use of TR-hepcidin revealed that hepcidin is degraded with kinetics similar to that of Fpn-GFP upon internalization. Addition of lysosome inhibitors prevented the degradation of TR-hepcidin and Fpn-GFP, indicating that the lysosome is the main site for the endocytic proteolysis of hepcidin and ferroportin. In addition, experiments with radiolabeled [^{125}I]M21Y-hepcidin indicated that internalized hepcidin is released by Fpn-GFP-expressing cells mostly as degraded forms of hepcidin-25. Thus, internalized hepcidin rarely undergoes lysosomal recycling and reutilization.

Fluorescent hepcidin could be employed *in vivo* to identify Fpn-expressing tissues and organs in whole organisms. Such derivatives will also be beneficial in designing hepcidin agonists and antagonists that are currently being investigated for the management of iron loading disorders and the anemia of chronic disease.

AUTHOR INFORMATION

Corresponding Author

*Chemical Biology Group, Institute of Pharmaceutical Sciences, King's College London, Franklin-Wilkins Building, 150 Stamford St., London SE1 9NH, U.K. E-mail: sukhi.bansal@kcl.ac.uk. Phone: +44(0)20 7848 4785.

Notes

The authors declare no competing financial interest.

REFERENCES

(1) Ganz, T. (2011) Hepcidin and iron regulation, 10 years later. *Blood 117*, 4425−4433.

(2) Pigeon, C., Ilyin, G., Courselaud, B., Leroyer, P., Turlin, B., Brissot, P., and Loreal, O. (2001) A new mouse liver-specific gene, encoding a protein homologous to human antimicrobial peptide hepcidin, is overexpressed during iron overload. *J. Biol. Chem. 276*, 7811−7819.

(3) Knutson, M. D., Oukka, M., Koss, L. M., Aydemir, F., and Wessling-Resnick, M. (2005) Iron release from macrophages after erythrophagocytosis is up-regulated by ferroportin 1 overexpression and down-regulated by hepcidin. *Proc. Natl. Acad. Sci. U.S.A. 102*, 1324−1328.

(4) Latunde-Dada, G. O., Vulpe, C. D., Anderson, G. J., Simpson, R. J., and McKie, A. T. (2004) Tissue-specific changes in iron metabolism genes in mice following phenylhydrazine-induced haemolysis. *Biochim. Biophys. Acta 1690*, 169−176.

(5) Laftah, A. H., Ramesh, B., Simpson, R. J., Solanky, N., Bahram, S., Schumann, K., Debnam, E. S., and Srai, S. K. S. (2004) Effect of hepcidin on intestinal iron absorption in mice. *Blood 103*, 3940−3944.

(6) Frazer, D. M., Wilkins, S. J., Becker, E. M., Vulpe, C. D., McKie, A. T., Trinder, D., and Anderson, G. J. (2002) Hepcidin expression inversely correlates with the expression of duodenal iron transporters and iron absorption in rats. *Gastroenterology 123*, 835−844.

(7) Nemeth, E., Tuttle, M. S., Powelson, J., Vaughn, M. B., Donovan, A., Ward, D. M., Ganz, T., and Kaplan, J. (2004) Hepcidin regulates cellular iron efflux by binding to ferroportin and inducing its internalization. *Science 306*, 2090−2093.

(8) Wang, R. H., Li, C. L., Xu, X. L., Zheng, Y., Xiao, C. Y., Zerfas, P., Cooperman, S., Eckhaus, M., Rouault, T., Mishra, L., and Deng, C. X. (2005) A role of SMAD4 in iron metabolism through the positive regulation of hepicidin expression. *Cell Metab. 2*, 399−409.

(9) Milward, E., Johnstone, D., Trinder, D., Ramm, G., and Olynyk, J. (2007) The nexus of iron and inflammation in hepcidin regulation: SMADs, STATs, and ECSIT. *Hepatology 45*, 253−256.

(10) Ross, S. L., Tran, L., Winters, A., Lee, K. J., Plewa, C., Foltz, I., King, C., Miranda, L. P., Allen, J., Beckman, H., Cooke, K. S., Moody, G., Sasu, B. J., Nemeth, E., Ganz, T., Molineux, G., and Arvedson, T. L. (2012) Molecular Mechanism of Hepcidin-Mediated Ferroportin Internalization Requires Ferroportin Lysines, Not Tyrosines or JAK-STAT. *Cell Metab. 15*, 905−917.

(11) Nemeth, E., and Ganz, T. (2006) Regulation of iron metabolism by hepcidin. *Annu. Rev. Nutr. 26*, 323−342.

(12) Park, C. H., Valore, E. V., Waring, A. J., and Ganz, T. (2001) Hepcidin, a urinary antimicrobial peptide synthesized in the liver. *J. Biol. Chem. 276*, 7806−7810.

(13) Jordan, J. B., Poppe, L., Haniu, M., Arvedson, T., Syed, R., Li, V., Kohno, H., Kim, H., Schnier, P. D., Harvey, T. S., Miranda, L. P., Cheetham, J., and Sasu, B. J. (2009) Hepcidin Revisited, Disulfide Connectivity, Dynamics, and Structure. *J. Biol. Chem. 284*, 24155−24167.

(14) Fernandes, A., Preza, G. C., Phung, Y., De Domenico, I., Kaplan, J., Ganz, T., and Nemeth, E. (2009) The molecular basis of hepcidin-resistant hereditary hemochromatosis. *Blood 114*, 437−443.

(15) Luo, X., Jiang, Q., Song, G., Liu, Y. L., Xu, Z. G., and Guo, Z. Y. (2012) Efficient oxidative folding and site-specific labeling of human hepcidin to study its interaction with receptor ferroportin. *FEBS J. 279*, 3166−3175.

(16) Abbate, V., Frascione, N., and Bansal, S. S. (2010) Preparation, Characterisation and Binding Properties of Molecularly Imprinted Hydrogels for the peptide hepcidin. *J. Polym. Sci., Part A: Polym. Chem. 48*, 1721−1731.

(17) Bansal, S. S., Halket, J. M., Fusova, J., Bomford, A., Simpson, R. J., Vasavda, N., Thein, S. L., and Hider, R. C. (2009) Quantification of hepcidin using matrix-assisted laser desorption/ionization time-of-flight mass spectrometry. *Rapid Commun. Mass Spectrom. 23*, 1531−1542.

(18) Clark, R. J., Tan, C. C., Preza, G. C., Nemeth, E., Ganz, T., and Craik, D. J. (2011) Understanding the Structure/Activity Relationships of the Iron Regulatory Peptide Hepcidin. *Chem. Biol. 18*, 336−343.

(19) Song, G., Jiang, Q., Xu, T., Liu, Y.-L., Xu, Z.-G., and Guo, Z.-Y. (2013) A convenient luminescence assay of ferroportin internalization to study its interaction with hepcidin. *FEBS J. 280*, 1773−1781.

(20) Preza, G. C., Pinon, R., Ganz, T., and Nemeth, E. (2013) Cellular Catabolism of the Iron-Regulatory Peptide Hormone Hepcidin. *PLoS One 8*, e58934.